Mechanism of Time-Dependent Inhibition of Polypeptide Deformylase by Actinonin

Glenn S. Van Aller,[#] Ravi Nandigama,[#] Chantal M. Petit,[#] Walt E. DeWolf, Jr.,[#,‡] Chad J. Quinn,[⊥] Kelly M. Aubart,[||] Magdalena Zalacain,[§] Siegfried B. Christensen,[||] Robert A. Copeland,[#] and Zhihong Lai*[,#]

Enzymology and Mechanistic Pharmacology, Microbiology, CASS, and Medicinal Chemistry, GlaxoSmithKline, 1250 South Collegeville Road, Collegeville, Pennsylvania 19426

Received June 30, 2004; Revised Manuscript Received September 20, 2004

ABSTRACT: Polypeptide deformylase (PDF) is an essential bacterial metalloenzyme responsible for the removal of the N-formyl group from the N-terminal methionine of nascent polypeptides. Inhibition of bacterial PDF enzymes by actinonin, a naturally occurring antibacterial agent, has been characterized using steady-state and transient kinetic methods. Slow binding of actinonin to these enzymes is observed under steady-state conditions. Progress curve analysis is consistent with a two-step binding mechanism, in which tightening of the initial encounter complex (EI) results in a final complex (EI*) with an extremely slow, but observable, off-rate ($t_{1/2}$ for inhibitor dissociation ≥0.77 days). Stopped-flow measurement of PDF fluorescence confirms formation of EI and provides a direct measurement of the association rate. Rapid dilution studies establish that the potency of actinonin is enhanced by more than 2000-fold upon tightening of EI to form EI*, from K_i = 530 nM (EI) to $K_i^* \leq 0.23$ nM (EI*). In sharp contrast, the previously reported small molecule PDF inhibitor, SB-543668, is a competitive, readily reversible inhibitor ($t_{1/2}$ for dissociation = 2.8 s). In addition, we demonstrate that BB-3497 is also a time-dependent inhibitor of PDF with an extremely slow off-rate. The two-step inhibition model detailed herein for the inhibition of *Staphylococcus aureus* PDF by actinonin and BB-3497 is consistent with a recent report on the time-dependent inhibition of *Escherichia coli* PDF by a macrocyclic peptidomimetic inhibitor [Ngugen, K. T., et al. (2004) *Bioorg. Chem.* 32, 178−191]. This study substantially extends our understanding of PDF inhibition and may facilitate the development of novel antibiotics.

The emergence of drug-resistant strains of pathogenic bacteria continues to be a serious threat to human health. New antibacterial agents, especially those with novel mechanisms of action, are urgently needed to tackle this important medical problem. In recent years, polypeptide deformylase (PDF)[1] has emerged as a promising new target for the development of such antibiotics (*1*, *2*).

Initiation of protein synthesis in bacteria requires formylation of the N-terminal methionine of methionyl-tRNA (Met-tRNA) by formyltransferase to produce f-Met-tRNA. After subsequent ribosomal translation of this molecular initiator, the majority of mature bacterial proteins must be N-deformylated by PDF, and then de-methionylated by bacterial methionine aminopeptidase, to be active (*2*, *3*). Genetic studies have shown that PDF is essential for bacterial survival (*4*). Although a putative human mitochondrial PDF has been identified and demonstrated to have a low level of catalytic activity, known inhibitors of the bacterial enzymes do not demonstrate toxicity toward human cell growth, except at extremely high concentrations (*5*−*8*). Hence, PDF is an attractive target for the development of novel, safe, broad-spectrum antibacterial agents.

Native bacterial PDF is a metallohydrolase that uses a ferrous ion (Fe^{2+}) to catalyze hydrolysis of the N-formyl group from the terminal methionine of nascent bacterial proteins. Atmospheric oxidation of Fe^{2+}-PDF makes it very unstable and difficult to work with in vitro (*9*, *10*). However, replacement of the bound iron by alternative divalent ions, such as Ni^{2+} and Co^{2+}, renders a highly stable enzyme that possesses activity and specificity virtually identical to those of the native ferrous form (*11*, *12*).

Recently, the antibacterial activity of actinonin has been attributed to its inhibition of PDF (*13*), with crystal structures confirming the binding of actinonin in the PDF active site (*14*). Using a formate-dehydrogenase coupled assay (*15*), we have established that actinonin is a slow-binding, competitive inhibitor of PDF enzymes from both Gram-positive and Gram-negative bacteria, as specifically illustrated herein for *Staphylococcus aureus* PDF. A two-step binding mechanism results in the tightening of the EI complex by more than 2000-fold. The resulting EI* complex has a very slow rate of dissociation of actinonin from the enzyme ($t_{1/2} \geq 0.77$ days), making it an extremely slowly reversible and non-covalent inactivator of PDF enzymes.

We have also compared actinonin with SB-543668, a competitive, rapidly reversible, small molecule PDF inhibitor,

* To whom correspondence should be addressed. Phone: 610-917-5171; fax: 610-917-7901; e-mail zhihong.v.lai@gsk.com.

‡ Current Address: Array Biopharma, 3200 Walnut St., Boulder, CO 80301.

Enzymology and Mechanistic Pharmacology.

§ Microbiology.

⊥ CASS.

|| Medicinal Chemistry.

[1] Abbreviations: PDF, polypeptide deformylase; f-MAS, *N*-formyl-methione-alanine-serine; FDH, formate dehydrogenase; NAD^+, nicotinamide adenine dinucleotide; NADH, nicotinamide adenine dinucleotide, reduced form; SAR, structure activity relationship.

10.1021/bi048632b CCC: $30.25
Published on Web 12/04/2004

and established that BB-3497, like actinonin, is a time-dependent PDF inhibitor with an extremely slow off-rate.

MATERIALS AND METHODS

Materials. Actinonin was purchased from Sigma. NAD^+ and FDH were obtained from Roche Diagnostics. *N*-Formyl-methionine-alanine-serine (f-MAS) was purchased from Bachem. All other chemicals were of highest commercial grade. SB-543668 was synthesized at GSK (*16*), with all PDF enzymes purified in their respective metallo forms by previously published methods (*16*). Enzymatic experiments reported herein were performed using *S. aureus* Ni^{2+}-PDF, unless otherwise specified.

Enzyme Assay and Inhibition Studies. PDF enzymatic activity was measured in a FDH-coupled assay (*15*). In this assay, the formate released by PDF from f-MAS is oxidized by FDH, thereby reducing one molecule of NAD^+ to NADH, and resulting in an increase in absorbance at 340 nm. To determine the inhibition constant (K_i) and IC_{50} values, reactions were initiated by adding PDF to 96-well microtiter plates containing all other reaction components. The final reaction composition was 2 nM PDF, 50 mM potassium phosphate, pH 7.6, 5 units/mL FDH, 15 mM NAD^+, and 10% DMSO, with the indicated concentrations of f-MAS and inhibitor. Initial reaction velocities were measured at 340 nm and 25 °C in a Molecular Devices SpectraMax plate reader.

Reversibility Studies. The reversibility of PDF inhibition was determined by two methods. To measure the rate of reactivation, enzyme and inhibitor were each incubated at 500 nM at room temperature for 15 min, and then diluted 200-fold into the FDH-coupled reaction mixture (the final concentration of both enzyme and inhibitor was 2.5 nM), as described under *Enzyme Assay and Inhibition Studies*. To determine whether actinonin binds to PDF covalently, actinonin and PDF were preincubated in 10 mM Tris pH 7.6 at concentrations of 20 and 40 μM in 250 μL, respectively. The enzyme mixture was then denatured by adding 4 volumes of a mixture of methanol and acetonitrile (1:1 by volume), and then lyophilized to dryness. Prior to LC/MS analysis, each sample was resuspended in 150 μL of water (Milli-Q 18 MΩ) containing 0.02% trifluoroacetic acid (TFA). A 5 μL aliquot of each sample was injected onto an analytical Porous R2/10 (2.1 × 100 mm) column at 60 °C, and eluted using a linear water/acetonitrile gradient at 0.5 μL/min. Mass spectra were obtained on a Waters LCT instrument using electrospray ionization (ESI).

Equilibrium Binding of Inhibitors to PDF Monitored by Intrinsic Tyrosine Fluorescence. Tyrosine-fluorescence spectra in the presence and absence of actinonin and SB-543668 were obtained using a Perkin-Elmer LS50B spectrometer. Emission spectra were recorded from 290 to 390 nm using an excitation wavelength of 275 nm.

Initial Binding of Inhibitors to PDF Measured by Transient Kinetic Methods. Pre-steady-state kinetics of inhibitor binding was measured by monitoring the decrease of tyrosine fluorescence in a Hi-Tech stopped-flow apparatus. Excitation and emission wavelengths were at 275 and 305 nm, respectively. A glass cutoff filter of 305 nm was installed in front of the photomultiplier. An equal volume of PDF and inhibitor was rapidly mixed in sodium phosphate buffer (pH 7.6) at 25 °C. The final concentration of PDF was 0.5 μM, with the final concentrations of actinonin and SB-543668 varied from 1 to 10 or 15 μM. Kinetic data for inhibitor binding were fit to a single-exponential function using KIMSIM software.

Scheme 1: Inhibition Mechanism for Inhibitors with (A) One-Step Binding and (B) Two-Step Binding Modes

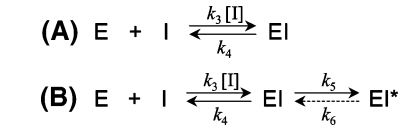

Berkeley Madonna software was used to model the population of different enzyme species for actinonin binding in the stopped-flow experiments. A two-step binding process represented by Scheme 1B was modeled using the kinetic constants for actinonin summarized in Table 1. The concentration of PDF was set at 0.5 μM, as in the stopped-flow experiments, with the actinonin concentration set at 5 and 1 μM for the simulation.

RESULTS

Progress Curve Analysis of PDF Inhibition by Actinonin and SB-543668. The peptidic hydroxamic acid actinonin has been reported to be a reversible PDF inhibitor with a K_i of 0.28 nM for *E. coli* Ni^{2+}-PDF and a similar K_i for *S. aureus* Ni^{2+}-PDF (*13*). We have reexamined actinonin inhibition of PDF using a FDH-coupled system (*12*, *15*) and compared actinonin with the nonpeptidic, N-formylhydroxylamine inhibitor, SB-543668 (*16*) (Figure 1). In the absence of inhibitor, product formation is linear with 2 nM *S. aureus* Ni^{2+}-PDF and 2.5 mM f-MAS (at K_m) for over 10 min (Figure 2A,B). In the presence of SB-543668, product formation is still linear, but the rates were reduced (Figure 2B). The IC_{50} of SB-543668 inhibition was determined to be 430 ± 26 nM.

In contrast, in the presence of actinonin, the progress curves for deformylation exhibit curvature consistent with a slow onset of inhibition (Figure 2A). The biphasic progress curves are well described by eq 1 (*17*, *18*).

$$[P] = v_s t + \frac{v_0 - v_s}{k_{obs}}(1 - e^{-k_{obs}t}) + Y_0 \qquad (1)$$

where v_0 is the initial reaction velocity, v_s is the final steady-state velocity, k_{obs} is the apparent first-order rate constant for the conversion between v_0 and v_s, and Y_0 is the background absorbance signal.

There are two basic kinetic mechanisms that could account for the slow-binding inhibition of enzyme-catalyzed reactions (*17*−*19*). Scheme 1A describes the simple one-step, reversible binding of inhibitor to enzyme. The slow onset of inhibition in this case results from the inherent slow rates of inhibitor association and, sometimes, dissociation for the EI binary complex. Scheme 1B depicts a two-step binding mechanism involving a tightening of EI to form EI*. Covalent and mechanism-based inhibitors can also follow a two-step mechanism, similar to Scheme 1B. To distinguish between binding Schemes 1A,B, we examined the effect of actinonin concentration on the apparent first-order rate constant k_{obs} (Figure 3). The rate of inactivation varied as a

Table 1: Kinetic Parameters of *S. aureus* Ni^{2+}-PDF Inhibition by SB-543668, Actinonin, and BB-3497

inhibitor	$k_3 \times 10^6$ ($M^{-1}s^{-1}$)	k_4 (s^{-1})	k_5 (s^{-1})	k_6 (s^{-1})	$t_{1/2}$	K_i (μM)	K_i^* (nM)
SB-543668	1.1 ± 0.1	0.25 ± 0.08	NA	NA	2.8 ± 1.0 s	0.22 ± 0.10[a]	NA[b]
actinonin	0.080 ± 0.010	0.042[c]	0.033 ± 0.001	$\leq 9.8 \times 10^{-6}$	≥ 0.77 days	0.53 ± 0.04[d]	≤ 0.23[e]
BB-3497	0.090 ± 0.001	0.14[c]	0.036 ± 0.003	$\leq 4.3 \times 10^{-6}$	≥ 1.9 days	1.5 ± 0.12[d]	≤ 0.18[e]

[a] K_i is from the average of both steady-state (based on v_o) and pre-steady-state measurements. [b] NA = not applicable. [c] Estimated based on $k_{off} = K_i k_{on}$. [d] K_i is determined from steady-state analysis using initial velocity. [e] Estimated using eq 5 and the upper limit determined for k_6.

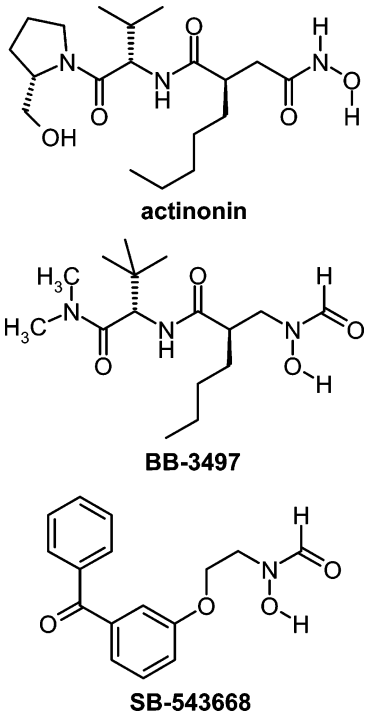

FIGURE 1: Chemical structures of actinonin, BB-3497, and SB-543668.

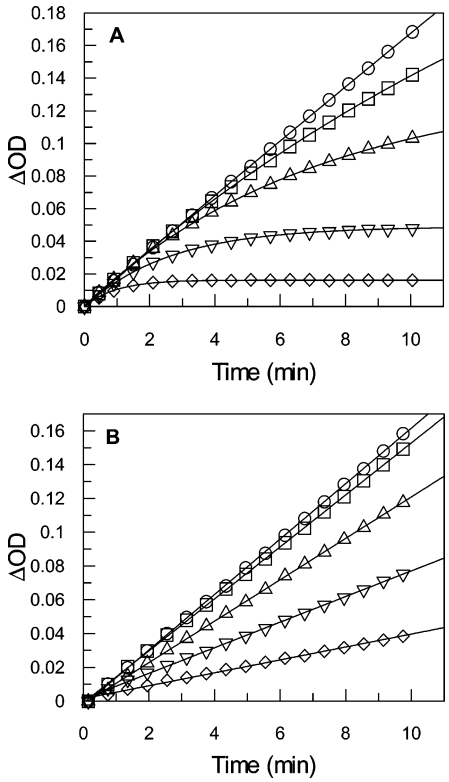

FIGURE 2: (A) Representative reaction time courses for *S. aureus* Ni^{2+}-PDF activity in the absence (○) and presence of 15 nM (□), 46 nM (△), 140 nM (▽), and 410 nM (◇) actinonin. (B) Reaction time courses for the uninhibited control (○) and reactions with 46 nM (□), 140 nM (△), 410 nM (▽), and 1.2 μM (◇) of SB-543668. Reactions were initiated by the addition of PDF, and activity was monitored by the FDH-coupled assay as described under Materials and Methods. All reactions contained 2.5 mM f-MAS. Data were fitted to eq 1 as described under Results.

hyperbolic function of [I], consistent with the two-step binding mechanism illustrated in Scheme 1B.

Since the steady-state velocity for the actinonin-inhibited reaction is essentially zero, actinonin acts, for all practical purposes, like an irreversible inactivator of the enzyme. The value of k_{obs} at different actinonin concentrations was fitted to eq 2 (*18*), fixing k_6 at zero. If k_6 was allowed to float, the value determined from the fitting was also extremely small, and not significantly different from zero.

$$k_{obs} = k_6 + \frac{k_5[I]}{K_i^{app} + [I]} \quad (2)$$

where K_i^{app} is the apparent K_i, which is related to the true K_i in different ways, depending on the mode of inhibition. Since the k_6 value is close to zero, the K_i^{app} in eq 2 no longer reflects the simple dissociation constant for the EI complex. Rather, K_i^{app} is defined as the apparent concentration of inhibitor required to reach half-maximal rate of inactivation of enzyme (K_I). Rate constant k_5, for the conversion of the initial EI complex to EI*, reflects the maximal rate of inactivation (k_{inact}) (*17*). For the inhibition of *S. aureus* Ni^{2+}-PDF by actinonin, k_{inact} and K_I were determined to be 0.033 $\pm$ 0.001 s^{-1} and 0.54 $\pm$ 0.07 μM, respectively.

Mode of Inhibition by Actinonin and SB-543668. The mechanism of actinonin inhibition toward *S. aureus* Ni^{2+}-PDF was determined by measuring k_{obs}, the apparent first-order rate constant for the onset of inhibition, at a fixed concentration of inhibitor and varying f-MAS concentrations (Figure 4). As the concentration of f-MAS increases, the decrease of k_{obs} can be well described by eq 3 (*18*), suggesting that actinonin is competitive with the f-MAS substrate.

$$k_{obs} = \frac{k}{1 + \frac{[S]}{K_m}} \quad (3)$$

where [S] is the concentration of f-MAS, K_m is the Michaelis constant for f-MAS, and k is the maximum value of k_{obs} when [S] = 0.

To obtain the inhibition constant (K_i) for the initial binding of actinonin, initial velocity (v_0) values were obtained from fitting the progress curves to eq 1. The v_0 values were then plotted at different actinonin concentrations as a function of substrate (Figure 5A). The double-reciprocal plot of actinonin

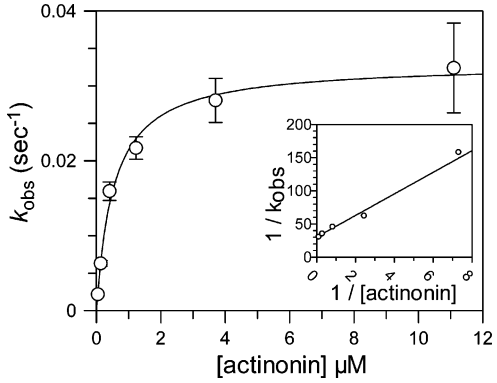

FIGURE 3: Dependence of k_{obs} (calculated from fitting the data in Figure 2A to eq 1) of *S. aureus* Ni^{2+}-PDF inactivation on actinonin concentration. Data from four independent measurements were averaged and fitted to eq 2. The inset contains a double-reciprocal plot of $1/k_{obs}$ as a function of 1/[actinonin].

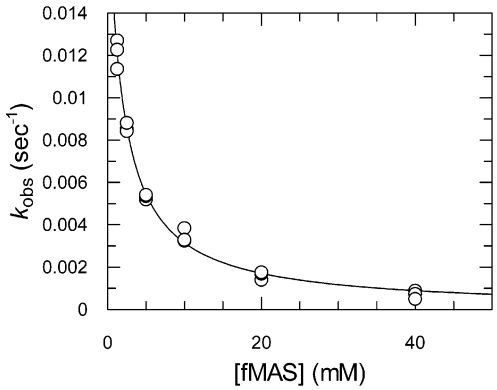

FIGURE 4: Dependence of k_{obs} (calculated from fitting progress curves to eq 1) of *S. aureus* Ni^{2+}-PDF inactivation by actinonin on substrate (f-MAS) concentration. The actinonin concentration was fixed at 167 nM. The solid line represents fitting three sets of data to eq 3.

inhibition showed a nest of lines converging on the *y*-axis, consistent with the competitive mode of inhibition (*18*). Fitting the data to eq 4, which describes competitive inhibition, the K_i was determined to be 0.53 ± 0.04 μM for actinonin, equivalent to the K_I value of 0.54 ± 0.07 μM derived above. Similarly, SB-543668 was found to be a competitive inhibitor of PDF with a K_i of 0.18 ± 0.03 μM. Since SB-543668 is not time dependent, initial velocities at different inhibitor concentrations were determined based on the slopes of the linear progress curves (Figure 5B).

$$v = \frac{V_{max}[S]}{K_m\left(1 + \frac{[I]}{K_i}\right) + [S]} \quad (4)$$

Reversibility of PDF Inhibition. Because our steady-state analysis unambiguously demonstrates that actinonin acts as an essentially irreversible PDF inhibitor, we conducted experiments to determine whether actinonin covalently modifies PDF. After incubation of actinonin with *S. aureus* Ni^{2+}-PDF, samples were denatured and analyzed by LC/MS as described in Materials and Methods. There was no mass change in either actinonin or PDF. The quantities of actinonin and PDF in the preincubated samples were essentially unchanged when compared to their respective controls by

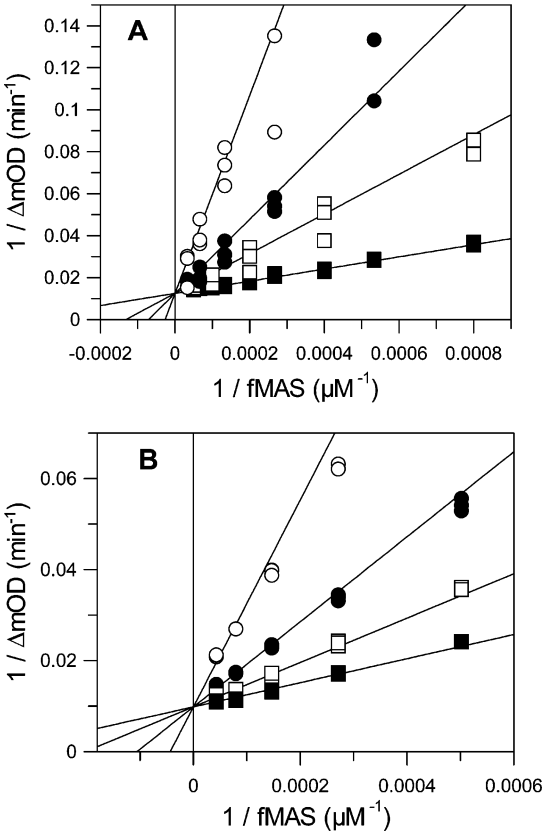

FIGURE 5: Double-reciprocal plots of the initial velocity (calculated from fitting each progress curve to eq 1) of *S. aureus* Ni^{2+}-PDF initiated reactions at (A) 0 (■), 1.2 μM (□), 2.7 μM (●), and 8.1 μM (○) actinonin and (B) 0 μM (■), 0.15 μM (□), 0.46 μM (●), 1.4 μM (○) SB-543668. The K_I values for actinonin and SB-543668, as well as the K_m for f-MAS, were determined by fitting three sets of data to eq 4.

LC analysis, suggesting that actinonin is not a covalent modifier of PDF (data not shown).

Strongly supporting this conclusion, the rate of dissociation of actinonin from *S. aureus* Ni^{2+}-PDF was measured in a rapid dilution experiment. After 500 nM PDF was incubated with 500 nM actinonin or SB-543668 for 15 min, samples were rapidly diluted by 200-fold into buffer containing a saturating amount of f-MAS substrate (10-fold of K_m) using the FDH-coupled assay. Under these conditions, SB-543668 inhibition was rapidly reversible and the recovered activity was indistinguishable from the control reaction preincubated only with DMSO (Figure 6A). The time required for SB-543668 to regain half-maximal enzyme activity ($t_{1/2}$) was too fast to be accurately determined by this method.

In contrast, enzyme preincubated with actinonin recovers only a small amount of activity after 2 h (Figure 6A,B). However, detailed inspection of the data indicated that the recovery of activity could be described by the exponential function defined by eq 1 (*17*). Because only a small fraction of activity was recovered by 2 h, we were not able to obtain a reliable steady-state velocity (v_s) value directly from the equation fitting. Thus, we attempted to fit the reactivation data in an iterative fashion, assuming that the reverse isomerization of EI* to EI is rate limiting to overall inhibitor dissociation ($k_6 \approx k_{obs}$). Initially, v_s was fixed at 100% of the DMSO control rate. The k_{obs} value obtained from the fitting of the reactivation experiment was used to calculate

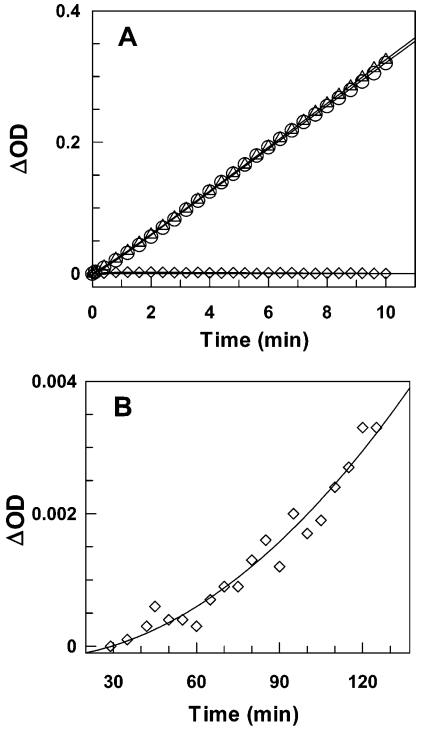

FIGURE 6: Kinetic traces for the reactivation of *S. aureus* Ni^{2+}-PDF after preincubation with inhibitors. Inhibitor and PDF were incubated at 0.5 μM each at room temperature for 15 min, and then diluted 200-fold into the FDH-coupled assay. Panel A displays product formation monitored by the absorbance changes over time after preincubation and rapid dilution in the presence of SB-543668 (○), DMSO control (△), and actinonin (◊). Panel B shows the extremely slow recovery of PDF activity after actinonin preincubation on a reduced *y*-axis scale. Solid lines represent the best fits to eq 1.

k_6 and K_i^* using eq 5, which were then used in eq 6 to predict the steady-state velocity v_s. Finally, the v_s value calculated from the fitting was used to fit eq 1 to obtain k_{obs} again, to start another cycle of fitting.

$$K_i^* = K_i \frac{k_6}{k_5 + k_6} \tag{5}$$

$$v_s = \frac{V}{\frac{K_m}{[S]}\left(1 + \frac{[I]}{K_i^*}\right) + 1} \tag{6}$$

where K_i^* is the overall inhibition constant defined by eq 5, V is the maximum velocity at $[I] = 0$, and [I] is the final inhibitor concentration after dilution. For this fitting, a K_i value of 0.53 μM, determined from mode of action analysis, and a k_5 value of 0.033 s^{-1}, from the progress-curve analysis, were used. Experimentally, $[S]/K_m$ and $[I]/K_i$ were 10 and 1/200, respectively.

After multiple iterations of these fittings (>10), k_{obs} converged to a single value of 9.8×10^{-6} s^{-1}. The final steady-state velocity, if we allow enough time for actinonin to fully dissociate from PDF, was predicted to be 42% of control velocity. Because k_{obs} has contributions from both k_6 and k_5 (*17*), k_6 was estimated to be $\leq 9.8 \times 10^{-6}$ s^{-1}. Therefore, actinonin's dissociation from EI* has a $t_{1/2} \geq 0.77$ days. While this dissociation rate is extremely slow, the observable recovery in activity, in conjunction with the unchanged mass spectral data, suggest that actinonin is a reversible and noncovalent inhibitor of PDF.

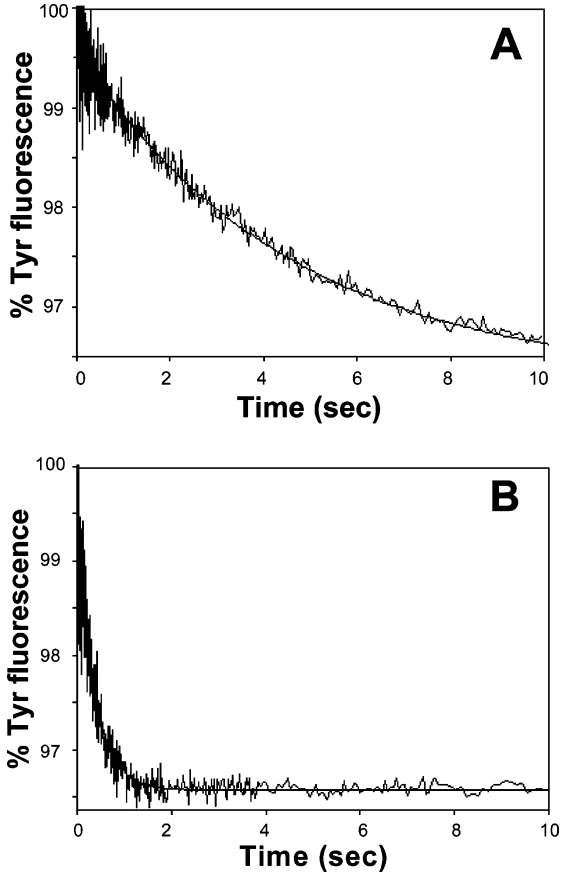

FIGURE 7: Representative pre-steady-state kinetic traces and best fits to a single-exponential function for 2.5 μM of (A) actinonin and (B) SB-543668 as measured in a stopped-flow apparatus following the decrease of tyrosine fluorescence of *S. aureus* Ni^{2+}-PDF upon inhibitor binding. Solid lines represent the best fit to a single-exponential decay.

Binding of Actinonin and SB-543668 to PDF by Equilibrium and Transient Kinetic Methods. Bacterial PDF enzymes from multiple organisms, including *E. coli*, *Haemophilus influenzae*, *Streptococcus pneumoniae*, and *S. aureus*, do not contain any tryptophan residues that can be used as a convenient spectroscopic handle to monitor binding. However, the Gram-positive bacteria *S. pneumoniae* and *S. aureus* PDFs contain a tyrosine residue in the S3′ pocket of the active site (for nomenclature of protease active sites, refer to ref *20*). Since actinonin and SB-543668 both have substituents that bind to PDF in the S3′ pocket (*14*, *16*), it seemed likely that the tyrosine fluorescence spectrum could be perturbed by inhibitor binding. Indeed, binding of actinonin and SB-543668 to *S. aureus* Ni^{2+}-PDF resulted in a 20% decrease of tyrosine fluorescence at 300 nm.

To measure the k_{on} and k_{off} for the formation of EI (i.e., k_3 and k_4 in Scheme 1A&B), the change in tyrosine fluorescence upon actinonin and SB-543668 binding to *S. aureus* Ni^{2+}-PDF was followed with stopped-flow instrumentation. A reduction in tyrosine fluorescence was observed when 0.5 μM *S. aureus* Ni^{2+}-PDF was mixed with SB-543668 or actinonin, ranging from 1 to 15 μM. Each kinetic trace is well described by a single-exponential function (Figure 7A,B). The k_{obs} values displayed a linear dependence on inhibitor concentration and were fitted to eq 7 (Figure

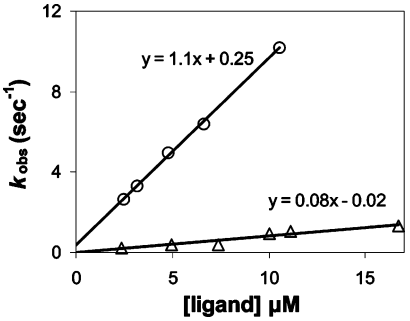

FIGURE 8: Dependence of k_{obs}, which represents the initial binding of actinonin (△) and SB-543668 (○) to PDF (determined from stopped-flow experiments), on inhibitor concentrations. Data were fitted to eq 7 to obtain k_{on} and k_{off} for the initial binding.

8), consistent with the hypothesis that the stopped-flow method measures EI formation, as defined in Scheme 1A for SB-543668 and Scheme 1B for actinonin.

$$k_{obs} = k_{on}[I]_{free} + k_{off} \quad (7)$$

For SB-543668, k_{on} and k_{off} for the formation of EI (i.e., k_3 and k_4 in Scheme 1A) were determined to be 1.1×10^6 M^{-1} s^{-1} and 0.25 s^{-1}, respectively. The initial K_i was calculated (as k_{off}/k_{on}) to be 0.26 μM, which is in very good agreement with the K_i of 0.18 μM determined from mode of action analysis using steady-state methods (average K_i = 0.22 μM, Table 1). The off-rate of 0.25 s^{-1} predicts a $t_{1/2}$ of 2.8 s for the dissociation of SB-543668 from PDF. This result is in very good agreement with our rapid-dilution experiment, in which the rate of reactivation for SB-543668 was too rapid to measure.

The initial binding of actinonin was analyzed similarly. The k_{on} for actinonin was determined to be 0.080×10^6 M^{-1} s^{-1}, indicating that actinonin forms EI 10-fold slower than SB-543668. It is also evident that k_{off} for actinonin is small and cannot be accurately determined directly from the fitting. Since the K_i of actinonin was determined to be 0.53 μM from mode of action analysis using initial velocity, we estimated k_{off} for actinonin to be 0.042 s^{-1}. Thus, the initial on- and off-rates for actinonin are significantly slower (10- and 5-fold, respectively) than the rates for SB-543668, while the K_i values for the EI complexes of PDF with actinonin and SB-543668 differ by only 2-fold.

Simulation of the Initial Binding of Actinonin to PDF. For time-dependent inhibitors with a two-step mechanism, it is commonly assumed that formation of EI is rapid, and is then followed by a slower isomerization reaction. However, the k_4 and k_5 values that we have estimated or measured for actinonin binding are very similar (0.042 and 0.033 s^{-1}, respectively). This means that during the initial time period after EI is formed, it has an equal chance to dissociate to E and I or to isomerize to EI*. Over time, all of the EI population will be transformed to EI*, due to the very slow off-rate of inhibitor from EI* (extremely small k_6). To understand whether the presence of the EI* species with an extremely slow off-rate affects our ability to measure the initial binding of actinonin (i.e., formation of EI from E and I) by stopped-flow methods, we have modeled the initial binding of actinonin using the rate constants listed in Table 1. Figure 9 represents the simulation with 0.5 μM PDF and 5 μM actinonin. In this simulation, E is rapidly depleted

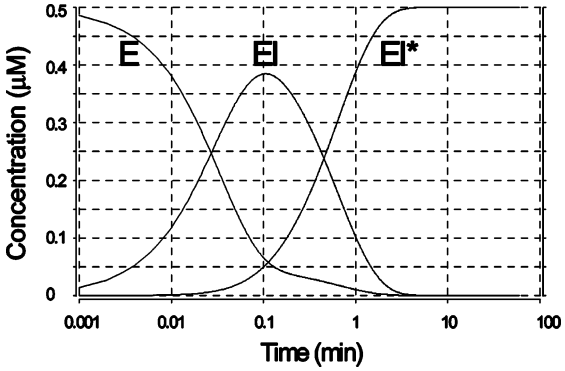

FIGURE 9: Simulation of the initial binding of actinonin to *S. aureus* Ni^{2+}-PDF following a two-step mechanism (Scheme 1B) uses Berkeley Madonna software. In this simulation, the total PDF and actinonin concentrations were set at 0.5 and 5.0 μM, with k_3, k_4, k_5, and k_6 values taken from Table 1.

during the initial time period to form EI. The concentration of EI peaks around 0.1 min, and then decreases due to the formation of EI*. The concentration of EI* is not significant until after 0.1 min, but all of EI is converted to EI* by 5 min. Within the 10 s time period of our stopped-flow experiments, we are primarily monitoring the formation of EI from E and I. Hence, the concentration of EI* is not significant during the stopped-flow measurement. Therefore, the presence of the EI to EI* transformation is not affecting our ability to measure the initial binding of PDF to actinonin under these conditions. We have also carried out simulations with 1 μM actinonin, in which formation of EI* is also not significant during the stopped-flow measurement.

Sculley et al. have presented a mathematical model for the two-step mechanism in which the initial interaction to form EI may not be much faster than the conversion from EI to EI* (*19*). The authors made the assumption that E is in equilibrium with EI and EI*. Under this circumstance, the steady-state progress curves should be fitted to a double-exponential function rather than a single-exponential function. There could be additional error associated with the values of K_i, k_5, and k_6 that are obtained from the steady-state progress curve analysis, when fitted to a single-exponential function. We have also attempted to fit our data to a double-exponential function but failed to obtain fits that were statistically better than the single-exponential fits. Notwithstanding, the value of k_6 was independently estimated using the rapid dilution experiment, and the value of k_3 was obtained from the transient kinetic measurements. Therefore, the accuracy of our estimates of k_3 and k_6 are not affected by the choice of fitting model for the progress curve analysis. Even if our determination of the k_4 and k_5 parameters were associated with higher errors, the data would still convincingly support the conclusion that actinonin binds with a two-step mechanism involving an extremely slow off-rate.

DISCUSSION

Our studies reveal that actinonin is a time-dependent inhibitor of PDF, with an extremely slow off-rate. We have also examined *S. pneumoniae*, *E. coli*, and *H. influenzae* Ni^{2+}-PDF, and the results are very similar to *S. aureus* Ni^{2+}-PDF (data not shown). Furthermore, we compared *S. aureus* Ni^{2+}-PDF to the naturally occurring Fe^{2+}-PDF, and again, the results were extremely consistent with the analysis

reported here for *S. aureus* Ni^{2+}-PDF, indicating that the identity of the metal ion does not change the profile of PDF inhibitor binding. We chose to report our complete characterization of actinonin binding to *S. aureus* Ni^{2+}-PDF, given its additional amenability to study by transient kinetic methods (vide supra).

The mechanism of inhibition of actinonin, in comparison with the non-time-dependent small molecule inhibitor SB-543668, was characterized using both steady-state and pre-steady-state methods. Binding constants as well as individual rate constants are summarized in Table 1. In contrast to SB-543668, actinonin binds to PDF by a two-step mechanism. Comparing the kinetic parameters between SB-543668 and actinonin, the most distinguishing feature of actinonin's binding is the extremely slow off-rate from EI*. The initial binding constants (K_i) are similar for SB-543668 and actinonin. However, due to the conversion from EI to the much tighter EI* complex, the potency for actinonin is further enhanced by over 2000-fold. The difference in free energy between EI and EI* can be estimated from the ratio of dissociation constants for the two complexes

$$\Delta\Delta G = RT \ln \frac{K_i^*}{K_i} \quad (8)$$

where R is the ideal gas constant and T is the temperature in Kelvin. Thus, the free energy difference between EI and EI* was calculated to be -4.48 kcal/mol at 25 °C. This difference is large enough to drive all of EI to EI*, resulting in essentially irreversible inhibition of PDF by actinonin.

Currently, the structural basis for the time-dependent inhibition of PDF by actinonin is not clear. Crystal structures of bacterial PDF enzymes (including *S. aureus* PDF) with and without actinonin (*14*) (i.e., the structures of E and EI*) do not show any significant conformational changes, indicating that the difference between EI and EI* is very subtle. More detailed studies are ongoing to understand the structural basis of the time-dependency of PDF inhibition by actinonin and other molecules.

Actinonin has been described by Chen et al. as a potent, competitive, and reversible inhibitor of PDF (*13*). We have confirmed the competitive nature of actinonin in this study. While inhibition of PDF by actinonin is reversible, the dissociation rate from EI* is extremely slow, resulting in a significant enhancement of potency. Chen et al. did not observe time-dependent inhibition of PDF by actinonin. This apparent discrepancy is likely due to the difference in experimental design between that work and the current studies. For inhibitor analysis, Chen et al. incubated PDF with inhibitors for 10 min before initiating the reaction with substrate. We have initiated all relevant experiments with the addition of PDF enzyme, without any inhibitor preincubation. The initial binding of actinonin and conversion from EI to EI* is relatively rapid; for example, in our simulations (Figure 9), all PDF has been converted to EI* within 5 min. With the 10 min preincubation period, Chen et al. were measuring the overall potency (K_i^*) of actinonin. In fact, the reported K_i^* (0.28 nM) for actinonin against *E. coli* Ni^{2+}-PDF, and a similar value against *S. aureus* Ni^{2+}-PDF, agree well with our K_i^* estimate of ≤ 0.23 nM for *S. aureus* Ni^{2+}-PDF.

Using similar approaches, we have also characterized the *N*-formyl hydroxylamine PDF inhibitor BB-3497 (*21*). Similar to actinonin, BB-3497 is a time-dependent inhibitor with an extremely slow off-rate (Table 1). The value of k_6 was estimated to be $\leq 4.3 \times 10^{-6}$ s^{-1}, which gives rise to a $t_{1/2}$ for dissociation from EI* of ≥ 1.9 days. The initial K_i of 1.5 ± 0.12 μM is further enhanced by more than 5800-fold to an overall potency of ≤ 0.18 nM.

Grant et al. have described the slow binding behavior of a hydrazoic acid inhibitor of PDF (*22*). However, this hydrazoic acid appears to bind to PDF in a single-step mechanism (Scheme 1A), with an off-rate on the order of $0.001-0.004$ s^{-1} ($t_{1/2}$ for dissociation of 3−12 min, depending on the PDF enzyme form). Recently, Nguyen et al. characterized the slow-binding inhibition of PDF by a macrocyclic peptidomimetic (*23*). This compound was proposed to inhibit PDF by a two-step mechanism. The value of k_6 was measured to be 0.62×10^{-6} s^{-1}, resulting in a $t_{1/2}$ of ~3 h. Our mechanistic characterization of actinonin, SB-543668, and BB-3497 is consistent with the notion that inhibition of PDF can proceed through different mechanisms, such as described by Scheme 1A,B. In addition, we have confirmed the two-step mechanism for actinonin and BB-3497, using transient kinetic methods to directly measure the initial binding step.

A time-dependent inhibitor with an extremely slow off-rate, like actinonin, may be beneficial for drug development. Since EI* has an extremely slow off-rate, the potential substrate accumulation that eventually overcomes simple, competitive inhibition has no effect on the EI* to EI isomerization. Consequently, no significant reversal of inhibition is possible once the EI* complex has formed. Additionally, the slow off-rate of the compound translates into a long residence time on the target that can extend the efficacy of the molecule beyond its clearance rate from systemic circulation. Several antibiotics demonstrate an unexpectedly delayed regrowth of bacteria following temporary in vivo exposure, a phenomenon that has been dubbed the post-antibiotic effect (PAE) (*24*, *25*). PAEs may influence optimal dosage intervals, and compounds demonstrating a prolonged PAE may allow wider dosing intervals in clinical usage. Indeed, the PDF inhibitor BB-83698 has been found to give a prolonged PAE, providing the potential for once-daily dosing for the treatment of *S. pneumoniae* infections (*1*). While actinonin itself is not suitable as a drug because of its poor pharmacokinetic properties, other slow-binding inhibitors with improved in vivo profiles may prove useful for antibacterial chemotherapy.

The inhibition mechanism described here for actinonin and BB-3497 presents two opportunities to design better inhibitors of PDF. Since actinonin and BB-3497 are time-dependent inhibitors of PDF with extremely slow off-rates, the efficiency of inactivation is represented by k_{inact}/K_I ($k_{inact} = k_5$, as defined in eq 2). One potential way to improve upon these inhibitors is to increase the rate of inactivation. Alternatively, the initial binding affinity could be augmented. Using detailed kinetic analysis of inhibitors for SAR should greatly facilitate accurate assessment of the dual contributions from the initial binding and the inactivation step. Understanding these individual contributions to the overall potency of inhibition may shed new light on designing PDF inhibitors as novel antibiotics.

ACKNOWLEDGMENT

We thank Drs. Peter Tummino, Nino Campobasso, and Mark Hemling for helpful discussions. We also thank Stewart Pearson for providing purified *S. aureus* PDF, Dr. Andrew Benowitz for synthesizing SB-543668 for these studies, and Drs. Symon Erskine and Lusong Luo for assistance with the stopped-flow instrumentation.

REFERENCES

1. Waller, A. S., and Clements, J. M. (2002) Novel approaches to antimicrobial therapy: peptide deformylase, *Curr. Opin. Drug Discov. Dev. 5*, 785−792.
2. Giglione, C., Pierre, M., and Meinnel, T. (2000) Peptide deformylase as a target for new generation, broad spectrum antimicrobial agents, *Mol. Microbiol. 36*, 1197−1205.
3. Solbiati, J., Chapman-Smith, A., Miller, J. L., Miller, C. G., and Cronan, J. E., Jr. (1999) Processing of the N termini of nascent polypeptide chains requires deformylation prior to methionine removal, *J. Mol Biol. 290*, 607−614.
4. Mazel, D., Pochet, S., and Marliere, P. (1994) Genetic characterization of polypeptide deformylase, a distinctive enzyme of eubacterial translation, *EMBO J. 13*, 914−923.
5. Giglione, C., Serero, A., Pierre, M., Boisson, B., and Meinnel, T. (2000) Identification of eukaryotic peptide deformylases reveals universality of N-terminal protein processing mechanisms, *EMBO J. 19*, 5916−5929.
6. Nguyen, K. T., Hu, X., Colton, C., Chakrabarti, R., Zhu, M. X., and Pei, D. (2003) Characterization of a human peptide deformylase: implications for antibacterial drug design, *Biochemistry 42*, 9952−9958.
7. Serero, A., Giglione, C., Sardini, A., Martinez-Sanz, J., and Meinnel, T. (2003) An unusual peptide deformylase features in the human mitochondrial N-terminal methionine excision pathway, *J. Biol. Chem. 278*, 52953−52963.
8. Lee, M. D., Antczak, C., Li, Y., Sirotnak, F. M., Bornmann, W. G., and Scheinberg, D. A. (2003) A new human peptide deformylase inhibitable by actinonin, *Biochem. Biophys. Res. Commun. 312*, 309−315.
9. Rajagopalan, P. T., and Pei, D. (1998) Oxygen-mediated inactivation of peptide deformylase, *J. Biol. Chem. 273*, 22305−22310.
10. Rajagopanlan, P. T., Yu, X. C., and Pei, D. (1997) Peptide deformylase: a new type of mononuclear iron protein, *J. Am. Chem. Soc. 119*, 12418−12419.
11. Ragusa, S., Blanquet, S., and Meinnel, T. (1998) Control of peptide deformylase activity by metal cations, *J. Mol Biol. 280*, 515−523.
12. Groche, D., Becker, A., Schlichting, I., Kabsch, W., Schultz, S., and Wagner, A. F. (1998) Isolation and crystallization of functionally competent *Escherichia coli* peptide deformylase forms containing either iron or nickel in the active site, *Biochem. Biophys. Res. Commun. 246*, 342−346.
13. Chen, D. Z., Patel, D. V., Hackbarth, C. J., Wang, W., Dreyer, G., Young, D. C., Margolis, P. S., Wu, C., Ni, Z. J., Trias, J., White, R. J., and Yuan, Z. (2000) Actinonin, a naturally occurring antibacterial agent, is a potent deformylase inhibitor, *Biochemistry 39*, 1256−1262.
14. Guilloteau, J. P., Mathieu, M., Giglione, C., Blanc, V., Dupuy, A., Chevrier, M., Gil, P., Famechon, A., Meinnel, T., and Mikol, V. (2002) The crystal structures of four peptide deformylases bound to the antibiotic actinonin reveal two distinct types: a platform for the structure-based design of antibacterial agents, *J. Mol. Biol. 320*, 951−962.
15. Lazennec, C., and Meinnel, T. (1997) Formate dehydrogenase-coupled spectrophotometric assay of peptide deformylase, *Anal. Biochem. 244*, 180−182.
16. Smith, K. J., Petit, C. M., Aubart, K., Smyth, M., McManus, E., Jones, J., Fosberry, A., Lewis, C., Lonetto, M., and Christensen, S. B. (2003) Structural variation and inhibitor binding in polypeptide deformylase from four different bacterial species, *Protein Sci. 12*, 349−360.
17. Morrison, J. F., and Walsh, C. T. (1988) The behavior and significance of slow-binding enzyme inhibitors, *Adv. Enzymol. Relat. Areas Mol. Biol. 61*, 201−301.
18. Copeland, R. A. (2000) *Enzymes: a Practical Introduction to Structure, Mechanism, and Data Analysis*, 2nd ed., Wiley, New York.
19. Sculley, M. J., Morrison, J. F., and Cleland, W. W. (1996) Slow-binding inhibition: the general case, *Biochim. Biophys. Acta 1298*, 78−86.
20. Barrett, A. J., Rawlings N. D., and Woessner J. F. (1998) *Handbook of Proteolytic Enzymes*, Acdemic Press, London, UK.
21. Clements, J. M., Beckett, R. P., Brown, A., Catlin, G., Lobell, M., Palan, S., Thomas, W., Whittaker, M., Wood, S., Salama, S., Baker, P. J., Rodgers, H. F., Barynin, V., Rice, D. W., and Hunter, M. G. (2001) Antibiotic activity and characterization of BB-3497, a novel peptide deformylase inhibitor, *Antimicrob. Agents Chemother. 45*, 563−570.
22. Grant, S. K., Green, B. G., and Kozarich, J. W. (2001) Inhibition and structure−activity studies of methione hydroxamic acid derivatives with bacterial peptide deformylase, *Bioorganic Chem. 29*, 211−222.
23. Nguyen, K. T., Hu, X., and Pei, D. (2004) Slow-binding inhibition of peptide deformylase by cyclic peptidomimetics as revealed by a new spetrophotometric assay, *Biorg. Chem. 32*, 178−191.
24. Spivey, J. M. (1992) The postantibiotic effect, *Clin. Pharm. 11*, 865−875.
25. MacKenzie, F. M., and Gould, I. M. (1993) The post-antibiotic effect, *J. Antimicrob. Chemother. 32*, 519−537.

BI048632B